LASER INTERFEROMETER GRAVITATIONAL WAVE OBSERVATORY
- LIGO -
CALIFORNIA INSTITUTE OF TECHNOLOGY
MASSACHUSETTS INSTITUTE OF TECHNOLOGY

Technical Note **LIGO-T1000300-v3** 2011/03/09

Advanced LIGO Transmon beam dump

J Fishner and S J Waldman

California Institute of Technology
LIGO Project, MS 18-34
Pasadena, CA 91125
Phone (626) 395-2129
Fax (626) 304-9834
E-mail: info@ligo.caltech.edu

Massachusetts Institute of Technology
LIGO Project, Room NW22-295
Cambridge, MA 02139
Phone (617) 253-4824
Fax (617) 253-7014
E-mail: info@ligo.mit.edu

LIGO Hanford Observatory
Route 10, Mile Marker 2
Richland, WA 99352
Phone (509) 372-8106
Fax (509) 372-8137
E-mail: info@ligo.caltech.edu

LIGO Livingston Observatory
19100 LIGO Lane
Livingston, LA 70754
Phone (225) 686-3100
Fax (225) 686-7189
E-mail: info@ligo.caltech.edu

`http://www.ligo.caltech.edu/`

1 Introduction

The beam transmitted through the Advanced LIGO End Test Masses (ETMs) is sensed using a pair of quadrant photodiodes (QPDs). In order to provide a sufficiently low noise signal, the QPDs are isolated on a suspended platform mounted to the ETM's seismic isolation stack. The suspended platform includes a beam reducing telescope to match the arm cavity beam to the QPDs. In order to reduce scattering, the ETM transmitted light that is not sensed by the QPDs will be dumped in a high quality beam dump mounted directly to the isolated platform. Finally, the suspended platform will have a dichroic optic and two QPDs for use with a 532 nm laser during the lock acquisition procedure. The suspended platform together with the QPDs, telescope, beam dumps and optics make up the aLIGO Transmission Monitor, a.k.a. Transmon. This note describes the basic calculations for the Transmon beam dump that specify its performance.

A schematic of the beam dump design is shown in Fig. 1.

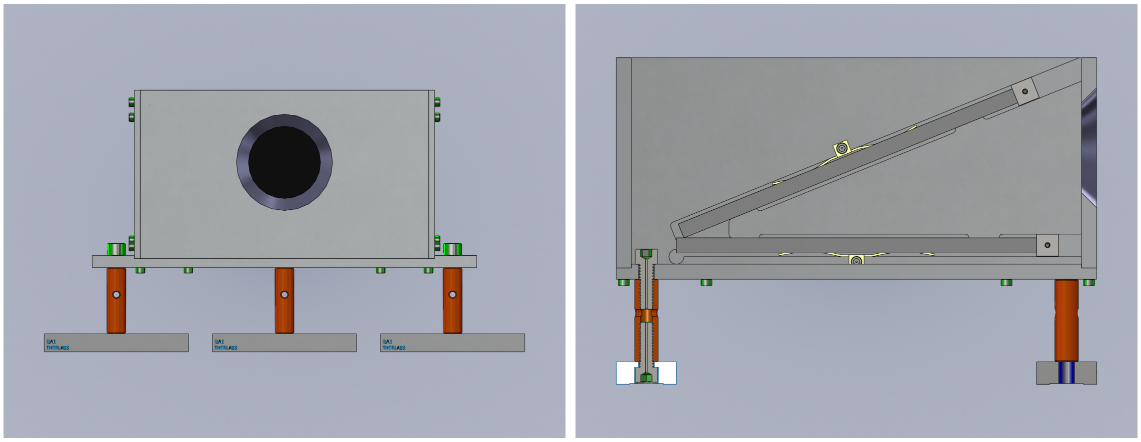

Figure 1: A schematic of the beam dump to be used in the calculations below. The two beam dump plates are mounted with poor thermal conduction to the enclosing box.

References

[1] **T070247-v1** ISC group; *AdvLIGO Interferometer Sensing and Control Conceptual Design*

[2] **D0902838-v2** P. Fritschel and E. Gustafson; *Advanced LIGO H1 Optical Layout*

[3] **LIGO-T0900486-v2** R. Martin and emphet al.; *IO Stray Light Analysis and Baffle Design*

[4] **New Semiconductor Materials electronic archive**

[5] C.P. Cagran and *et al.*; *Temperature-Resolved Infrared Spectral Emissivity of SiC and Pt10Rh for Temperatures up to 900C* Int. J. of Thermophysics Vol. 28.

[6] **T0900385** S J Waldman; *The Advanced LIGO ETM transmission monitor*

2 Silicon carbide

We will use silicon carbide (SiC) as the scattering surface in the transmon beam dump. The University of Florida IO group has evaluated SiC for use as a high power beam dump and beam baffle in the input path and found to have very low scatter and high power handling capabilities [3]. As an extremely strong ceramic material, SiC can be super-polished (to reduce scatter), has high thermal conductivity, and is much stronger than the commonly used welder's glass. In testing for the IO baffles, a SiC beam dump absorbed an 80 W, 1.4 mm beam with no signs of damage. A 200 μm beam created a visible spark and surface damage, but did not structurally compromise the beam dump. As a substrate, SiC will easily handle the 5 W, 2 mm radius Transmon beam.

In Fig. 2, we reproduce data from Rodica Martin for a measurement with "about 100 mW laser power and with a 1.4 mm beam diameter." The background light corrected reflectivity at Brewster's angle is 300 ppm.[1] David Feldbaum measured 260 ppm with an 85 W beam.[2] At this time, BRDF data is not available. Liyuan Zhang measured an unpolished SiC substrate from some manufacturer using the Caltech scatterometer for both polarizations. The data is shown in Fig. 3 and shows a comparable BRDF for both polarizations at the level of $3 \times 10^{-3} sr^{-1}$. Note that the reflectivity of the forward going beam, $\approx 27\%$, is a factor of 2 lower than the value measured in Figure 2, and may be a result of the scattering into large angles.

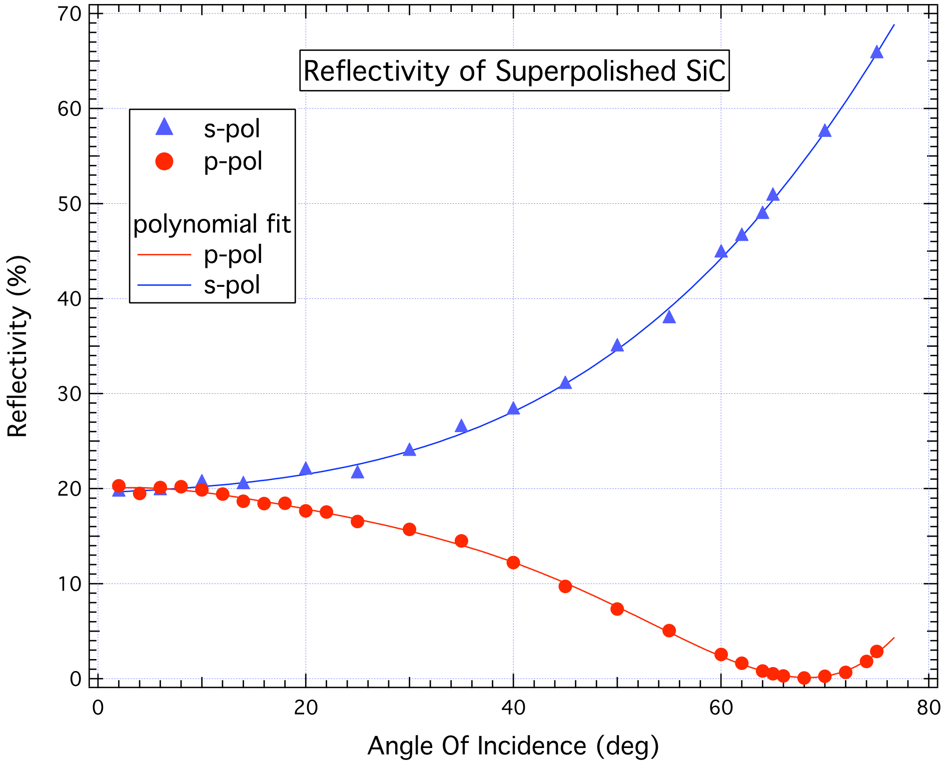

Figure 2: Measured reflectivity of a super-polished SiC beam dump.

---

[1] From an April 23, 2010 email between R. Martin and SJW.

[2] From the same email.

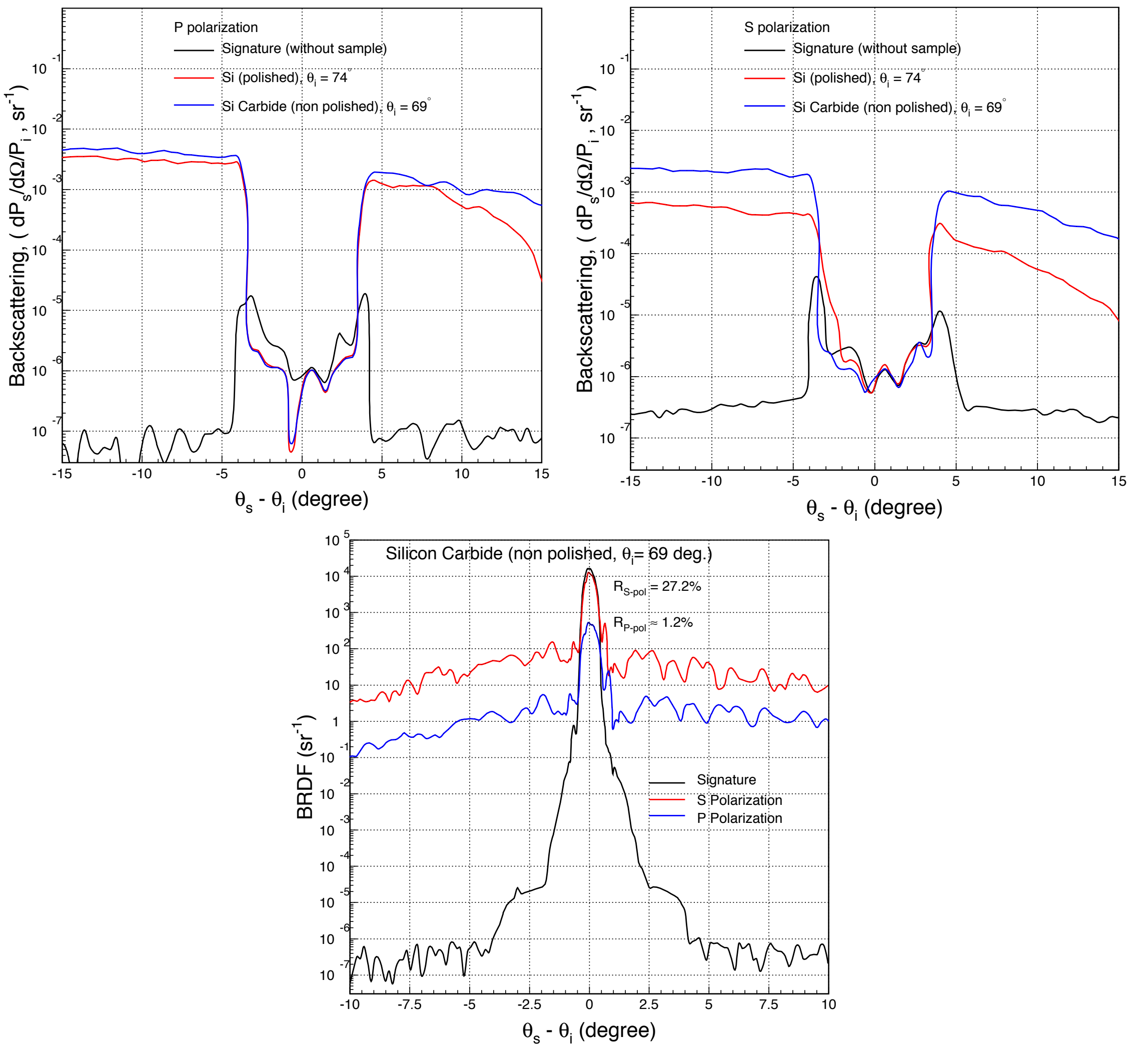

Figure 3: Measured BRDF and forward scattering of an unpolished SiC substrate in both polarizations. Data courtesy Liyuan Zhang.

From the data in Fig. 2 and 3 and listed references, we tabulate the relevant properties of SiC in Table 1.

Property	Value	Units	Reference
Density	3.16	g/cc	[4]
Elastic modulus	501	GPa	[4]
Thermal conductivity	3.6	W / cm K	[4]
Thermal expansion	3.8	10^{-6} / C	[4]
Emissivity	0.8		[5]
Specific heat	0.69	J /g K	[4]
Index @ 1064	2.575		[4]
Brewster's angle	68.8	degrees	

Table 1: Material properties of silicon carbide.

3 Input parameters

The beam dump should not be the limiting aperture for the incident 1064 nm beam. Instead, we assume that the input beam is reflected from a 2 inch diameter mirror at 45 degrees. The beam could be either horizontal or vertical polarization. For the Transmon table, the beam is horizontal polarization. Two maximize the number of reflections in the beam dump, the plates are mounted at a shallow angle, approximately 70 degrees. The plate must have an aperture of 2 inches, so it has a linear dimension of at least $L \times cos 68.8 deg. = 2\ inch; L = 5.5\ in.$ We round up and specify a 6 × 6 inch SiC plate. To maximize the beam dump efficiency, it will have two plates in a wedge.

The ETM transmission is specified as 5 ppm. The interferometer will have a maximum build up power of $\approx 750\ kW$. The beam dump will be required to dissipate all but a few milliwatts of the 3.8 W transmitted in continuous duty. Again we round up and specify a dissipation of 5 W. Because of the tight alignment tolerances of the transmon telescope, we minimize the heat flow into the transmon table. Instead, we radiate the majority of heat way from the transmon table to the vacuum chamber walls.

4 Thermal load

To model the thermal properties of the beam dump, we assume thatw the power dissipation is purely radiative and that the SiC plate has low thermal conductivity to the mount. In effect, only the top-most plate radiates to the vacuum chamber, and only from the top surface. The total radiating surface area is $A = 230\ cm^2$. Assuming an ambient temperature of $T = 295\ K$, the temperature rise of the isolated beam dump plate is

$$\delta T \approx \frac{\delta P}{4 \sigma A \epsilon, T^3}, \tag{1}$$

$$= 46\ K. \tag{2}$$

Here, $\sigma = 5.67 \times 10^{-8} W/m^2 K^4$ is the Stefan-Boltzmann constant and $\epsilon_{SiC} = 0.8$ is the emissivity of the SiC plate at 295 K. This temperature rise is an overestimate because all the radiation will not be limited to the beam dump plate and the temperature rise is large enough to merit a (negative) correction to the approximation used in Eq. 1.

To avoid heating the transmon table, the three 1.38 inch legs supporting the beam dump must be able to maintain the 46 K temperature gradient. We require the legs to dissipate less than 10% of the total power, $P_{legs} = 500\ mW$. Assuming standard thermal conduction, the thermal conductivity must satisfy:

$$k_{leg} \leq \frac{L}{dT\ A_{legs}} P_{legs} \tag{3}$$

$$\leq 6.4\ W\, m^{-1}\, K^{-1}. \tag{4}$$

For comparison, steel has a thermal conductivity of 16, Macor 1.5, and PEEK 0.25 $W\, m^{-1}\, K^{-1}$. We will use Macor or PEEK for the legs and thus we can neglect conduction to the table.

To estimate the radiative heat loss into the table, we assume the beam dump only radiates heat vertically. Following the schematic in Fig. 1, we see there are two layers between the primary beam dump plate and the table, and all have approximately equal areas. We model the system as three equal area plates, each radiating to the layer immediately above and below. The top most SiC plate has a power input of 5 W, which it then radiates equally up into the environment and down into the central plate. The central SiC plate reaches an equilibrium radiating and absorbing equal powers in both directions. The lowest aluminum plate radiates upwards and down into the table. The total power radiated by the i-th plate is $2P_i$; the plate radiates P_i W upwards and P_i W downwards. The top two plates are silicon carbide, with an emissivity of $\epsilon_{SiC} = 0.8$. The lowest plate has the emissivity of aluminum which we take to be $\epsilon_{Al} \approx 0.1$ (which is probably high). A simple three element transport model looks like:

$$\begin{pmatrix} P_1 \\ P_2 \\ P_3 \end{pmatrix} = \begin{pmatrix} 0 & \frac{\epsilon_{SiC}}{1+\epsilon_{SiC}} & 0 \\ \frac{\epsilon_{SiC}}{\epsilon_{SiC}+\epsilon_{SiC}} & 0 & \frac{\epsilon_{SiC}}{\epsilon_{SiC}+\epsilon_{SiC}} \\ 0 & \frac{\epsilon_{Al}}{1+\epsilon_{SiC}} & 0 \end{pmatrix} + \begin{pmatrix} \frac{P_0}{1+\epsilon_2} \\ 0 \\ 0 \end{pmatrix} \tag{5}$$

and predicts that 0.25 W is radiated downwards from the lowest plate while 4.75 W is radiated upwards. This result is sensitive to the emissivity of the bottom aluminum plate. If in practice $\epsilon_{Al} = 0.25$, the power radiated downwards doubles. However, "polished" aluminum usually has emissivity values less than 0.1, thus we expect 0.25 W to be an upper limit.

5 Backscatter requirements

Back scattered light from the Transmon table should contribute less than 1/10th the apparent interferometer displacement at 10 Hz. Assuming the Transmon motion is less than one fringe, we neglect fringe wrapping and set the requirement that

$$x_s\, E_s < 0.1 \times x_{ifo}\, E_{ifo}\Big|_{f=10\ \mathrm{Hz}}. \tag{6}$$

To estimate the Transmon motion, we assume that the seismic isolation platform is moving $x_{isi} = 10^{-11}\ m/\sqrt{Hz}$ at 10 Hz. We model the Transmon suspension as a double suspension with two poles at 4 Hz, for a total isolation factor at 10 Hz of 30 (this is an underestimate). Thus, the displacements at 10 Hz are

$$\begin{aligned} x_s &= 3 \times 10^{-13}\ m, \text{ and} \\ x_{ifo} &= 6 \times 10^{-19}\ m. \end{aligned} \tag{7}$$

We consider primarily the case of a prompt back reflection of the arm cavity transmission beam, such that

$$E_s = T_{ETM}\sqrt{R_s}E_{ifo}, \text{ and} \tag{8}$$

$$\sqrt{R_s} < 0.1\frac{x_{ifo}}{T_{ETM}x_s}, \tag{9}$$

where T_{ETM} is the power transmissivity of the End Test Mass (two passes through the ETM) and R_s is the reflectivity of the scatterer (one reflection). The final requirement for the beam dump reflection is:

$$R_s < 1.6 \times 10^{-3}. \tag{10}$$

The infrared beam has a waist size of 3.1 mm, a divergence angle of 110 μrad, and subtends a solid angle of 3×10^{-8} sr. Assuming a BRDF of 3×10^{-3} sr^{-1} as shown in Figure 3, the reflectivity of the first bounce off silicon carbide will be $R_{SiC} \approx 10^{-10}$. Even assuming several bounces off SiC, this value is far lower than the requirement Eq. 10.

6 Geometry

SiC exceeds the required back-reflection requirements by many orders of magnitude. An appropriate geometry of SiC plates is used to prevent forward reflections from returning towards the interferometer. A Zemax ray-tracing of a beam dump is shown in Figure 4. The beam dump model is based on Figure 1 in which there is an aluminum front plate with a hole opening onto two SiC mounted at an angle. The model shows the central ray in blue, and beams at $\pm 12\ mm$ in red. The beam will take at least 7 bounces at a variety of angles before returning through to the input plane if the angle between the SiC plates is held to

$$\theta_{SiC} = 68.9 \pm 0.3\ degrees. \tag{11}$$

After 7 bounces, the beam is attenuated by a factor of 2×10^{-4}. Note that the return beam will be reflected off the front plate of the beam dump and continue to scatter in the beam dump. Nonetheless, even this pessimistic value of the reflectivity will meet the limits required by Eq. 10.

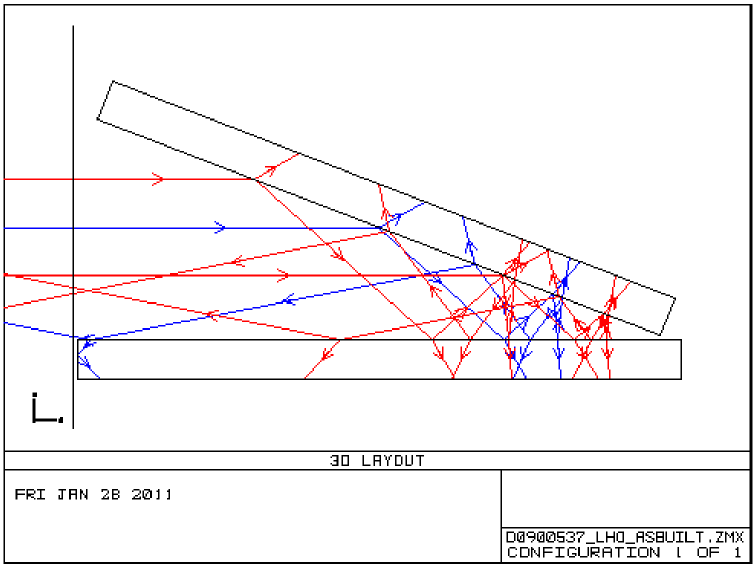

Figure 4: Zemax ray-tracing of the infrared beam. The beam takes at least 7 bounces before returning to the front plate.